AGU PUBLICATIONS

JGR

Journal of Geophysical Research: Atmospheres

RESEARCH ARTICLE
10.1002/2015JD023886

Key Points:
- RBT frequency changes can be mostly explained by the mean trend, while in summer also by variance
- The summer ratios increased during the hiatus period, while the winter ratios decreased
- Models are unable to reproduce the RBT asymmetry between TX and TN and hiatus characteristics

Supporting Information:
- Figures S1–S3
- Table S1

Correspondence to:
Z. Gao,
zgao@mail.iap.ac.cn

Citation:
Zhang, Y., Z. Gao, Z. Pan, D. Li, and B. Wan (2016), Record-breaking temperatures in China during the warming and recent hiatus periods, *J. Geophys. Res. Atmos.*, *121*, doi:10.1002/2015JD023886.

Received 2 JUL 2015
Accepted 4 DEC 2015
Accepted article online 12 DEC 2015

Record-breaking temperatures in China during the warming and recent hiatus periods

Yuanjie Zhang[1,2], Zhiqiu Gao[1,3], Zaitao Pan[2], Dan Li[4], and Bingcheng Wan[3]

[1]Collaborative Innovation Center on Forecast and Evaluation of Meteorological Disasters, Nanjing University of Information Science and Technology, Nanjing, China, [2]Department of Earth and Atmospheric Sciences, Saint Louis University, St. Louis, Missouri, USA, [3]State Key Laboratory of Atmospheric Boundary Layer Physics and Atmospheric Chemistry, Institute of Atmospheric Physics, Chinese Academy of Science, Beijing, China, [4]Program of Atmospheric and Oceanic Sciences, Princeton University, Princeton, New Jersey, USA

Abstract The observed and modeled record-breaking temperature (RBT) frequency in China is analyzed for different segments of the period 1961–2050 including the hiatus period. It is found that significant changes in the RBT frequency occurred earlier, with greater amplitude, for daily minimum temperatures (TN) compared to maximum temperatures (TX) during the past five decades. Changes in the RBT frequency can be mostly explained by the mean warming trend, especially for TN, while in summer also slightly by variance. Moreover, mean climate change affects more the multiday mean RBT than the single-day counterpart as RBT occurrence is inversely proportional to variance that is smaller for multiday means. In the hiatus period (1998–2013), the ratios of record highs to lows in summer continue to increase in southern China primarily due to the lower frequency of record lows, since the decreasing temperature variance suppressed the increase in record highs under the summer warming. While the winter ratios decreased significantly across most of the country due to the winter cooling. Model simulations show a much smaller asymmetry of the RBT frequency between TX and TN as compared to the observations. The 28-model median overestimates the ratios for TX owning to missing the relative cooling in the "warming hole" region and is unable to reproduce the RBT characteristics in the hiatus period. Under a high-emission scenario, increasing rates of future temperature extremes are projected to accelerate with almost doubling ratio trends in the first half of 21st century compared to the historical results.

1. Introduction

China has experienced significant warming in the twentieth century [*Ren et al*., 2012] consistent with the warming trend of the global climate [*Ji et al*., 2014]. Global warming is accompanied by not only increases in mean temperatures but also changes in frequency, intensity, duration, and spatial extent of extreme events such as extreme temperatures, heavy precipitations, and intense droughts, all of which have significant ecological, economic, and sociological consequences [*Coumou and Rahmstorf*, 2012]. In this study, we focus on temperature extremes in China using record-breaking temperature (RBT) [e.g., *Meehl et al*., 2009; *Xiong et al*., 2009; *Zhang et al*., 2009; *Pan et al*., 2013a] as an indicator of temperature extremes.

Recent studies have reported that extremely warm temperature events have increased significantly during the past decades as climate warms both globally [e.g., *Hansen et al*., 2012; *Donat and Alexander*, 2012; *Coumou et al*., 2013] and in China [e.g., *You et al*., 2011; *Zhou and Ren*, 2011; *Zhang et al*., 2011; *Wen et al*., 2013; *Sun et al*., 2014; *Zhou et al*., 2014]. Some previous studies support that a shift in the mean temperature is the main cause for the increase in temperature extremes [*Simolo et al*., 2011; *Donat and Alexander*, 2012]. *Wergen and Krug* [2010] concluded that the mean temperature trend has a moderate but significant contribution to the RBT frequency based on station data over European. *Trewin and Vermont* [2010] found that the frequency of RBT was broadly consistent with the mean annual temperature trend in Australia.

However, many other studies suggest that changes in the temperature variance are also an important contributor to the increase in temperature extremes [*Schär et al*., 2004; *Hansen et al*., 2012]. *Rahmstorf and Coumou* [2011] found that the RBT frequency increases approximately in proportion to the ratio of the mean temperature trend to the short-term standard deviation. Using weather station data collected during 1961–2004, *Pan et al*. [2013a] showed that a linear mean temperature trend could not explain the variability of RBT in China. Consequently, it is still unclear which of the two factors dominates increases in temperature

extremes. One of the objectives of our study is to examine contributions of varying temperature mean and variance to changes in temperature extremes using historical surface station data.

Understanding the impact of future climate change on temperature extremes requires the use of global climate model simulations such as those from the Coupled Model Intercomparison Project (CMIP) [*Kharin et al*., 2013; *Pan et al*., 2013a; *Wuebbles et al*., 2014]. Simulations from the fourth version of National Center for Atmospheric Research Community Climate System Model (CCSM4), one of the models included in CMIP5, show that the general trend and magnitude of RBT are in good agreement with observations in China [*Pan et al*., 2013a], whereas *Meehl et al*. [2009] reported that simulations of U.S. twentieth century climate from CCSM3 (i.e., the prior version of CCSM4) show a larger ratio of record high maximum to low minimum of daily temperatures than in observations, which is partly due to model's more uniform warming across the U.S. Warm temperature extremes are almost universally projected to become more frequent and more severe in the 21st century [*Kharin et al*., 2013; *Wuebbles et al*., 2014]. Based on the strongest representative concentration pathway (RCP8.5) scenario in CCSM4, the high maximum to low minimum record ratio over China by the middle-21st century with respect to 2006 could reach 6.8 [*Pan et al*., 2013a], much greater than the expected value of 1.0 in a stationary climate. In our study, we use multiple CMIP5 model simulations in 21st century to the present future RBT characteristics in China and validate simulation in twentieth century against surface station data. Although some previous studies have investigated RBT characteristics in China [e.g., *Xiong et al*., 2009; *Pan et al*., 2013a], RBT statistics based on multimodel simulations have not been studied.

The latest studies suggest that the global mean temperature has no statistically significant increase since 1998 [*Fyfe et al*., 2013; *Curry*, 2014], which has often been referred to as the global warming "hiatus" [*Meehl et al*., 2011]. In this study 1998–2013 is defined as the hiatus period. The cause of this hiatus has been the subject of active researches [e.g., *Meehl et al*., 2011, 2013]; however, less attention has been paid to the characteristics of extreme temperatures such as RBT statistics over the hiatus period. Recently, *Seneviratne et al*. [2014] reported that hot extremes show a continued increase over land during the hiatus period, whereas *Sillmann et al*. [2014] found that cold extremes exhibit a coherent cooling pattern across the Northern Hemisphere midlatitudes in the recent 15 years. Understanding changes in temperature extremes during the hiatus period not only offer insights into the impact of climate change on temperature extremes under different background climates but also shed light on how the future temperature extreme trend would be if the hiatus were to continue. In this study, we use up-to-date station observations in order to examine changes in temperature extremes during the hiatus period in China, which to the authors' knowledge has not been studied elsewhere. Also, different from previous studies in which only single-day record high maximum and low minimum temperatures were analyzed [e.g., *Meehl et al*., 2009; *Pan et al*., 2013a], this study computes single-day record highs and lows for both maximum and minimum temperatures in order to better compare warm to cold extremes. In addition, RBT analysis is also extended to multiday scales to investigate temperature extremes lasting several days.

2. Data

Observational data including daily maximum and minimum surface air temperatures, abbreviated as TX and TN, respectively, from 756 stations are provided by the National Meteorological Information Center, China Meteorological Administration (CMA). This data set, subjected to rigorous quality control, has an relatively complete coverage over China [e.g., *Zhai et al*., 2005; *Zhou and Ren*, 2011]. The number of stations increased from 180 to above 650 during 1951–1960 and maintained at this level since 1961 [*Pan et al*., 2013a]. To avoid effects from varying record lengths [*Meehl et al*., 2009], a uniform period, from 1961 to 2013, is chosen. Stations with more than 10% missing data are excluded from the analyses, and the missing data in remaining stations are filled in by a simple linear interpolation from values of neighboring days. There are 224 (285) stations that have missing TX (TN). The average missing rate over these stations is only 0.54% and 0.43% for TX and TN, respectively. So our results are unlikely to be affected by the linear interpolation method employed here.

A major challenge in assessing changes in observed temperatures is data inhomogeneity mainly associated with station relocation and/or changes in the surrounding environment. Our study uses the China Homogenized Historical Temperature data [*Li et al*., 2009; *Pan et al*., 2013a] for the period 1961–2004, and

the nonhomogenized data for the period 2005–2013. The data homogeneity for the whole period 1961–2013 is assessed by the RHtest of *Wang et al*. [2007] (http://etccdi.pacificclimate.org/software). After scrutiny, 64 stations with significant inhomogeneity are excluded. In addition, 55 stations in major urban centers (population over 1 million) are also excluded because of the potential urban heat island effect, although this effect on analyzed global change and local warming trend is found to be small [*Hansen et al*., 2010; *Trewin and Vermont*, 2010]. After the above quality control, a total of 532 stations are finally selected. These stations are distributed across the country but not uniformly. The number of stations in the western China is limited (e.g., see Figure 4).

Model-simulated daily TX and TN from CMIP5 are also used in this study [*Taylor et al*., 2012]. CMIP5 includes various experiments, and here we choose the *historical* experiments for the twentieth century under natural and anthropogenic forcing and the *projection* experiments for the 21st century under different RCPs scenarios, where RCP2.6, for example, indicates that the radiative forcing value is 2.6 W m^{-2} by 2100 [*Moss et al*., 2010]. In this study, we focus on the RCP8.5 scenario, which is the strongest warming scenario in CMIP5. Since only limited daily outputs are provided by participating models, most of which have only a single *historical* or RCP8.5 ensemble member, we use a single ensemble member from each model, mostly *r1i1p1* realization, for our analysis. In addition, since CMIP5 models have different numbers of simulated calendar days (360, 365, or 366), only those models with 365 or 366 (29 February for each year is ignored) calendar days are chosen. As a result, 28 models are selected in this study, as listed in Table S1 in the supporting information.

3. Methodology

The frequency of record-breaking high or low daily temperature is a measure of changes in temperature extremes [*Meehl et al*., 2009]. To compute the frequency of RBT, the daily TX (or TN) of each calendar day from 1961 to 2013 are first arranged into a 53 (row) × 365 (column) array. Then, the temperature on any specific day (e.g., 1 January) will be a RBT if it is higher or lower than any temperatures on the same day (i.e., 1 January) in previous years. In the first year, the number of RBTs is 365 at any station since there are no prior data, so all temperatures are RBTs. For subsequent years, the number of RBTs decreases as breaking the record becomes progressively difficult. Mathematically, in an independently and identically distributed and thus stationary series, the probability of record breaking with increasing years follows the 1/*n* curve, where *n* is the number of years [*Arnold et al.,* 1998]. In a nonstationary series, *Wergen and Krug* [2010] presented the probability of RBT with increasing years when the temperature has a linear warming trend:

$$p_n \approx \frac{1}{n} + \frac{v}{\sigma}\frac{2\sqrt{\pi}}{e^2}\sqrt{\ln\left(\frac{n^2}{8\pi}\right)}, \quad n \geq 7, \tag{1}$$

where v is the linear temperature trend and σ is the standard deviation over the analysis period, in °C yr^{-1} and °C, respectively. Without the linear trend (i.e., $v = 0$), equation (1) reduces to the 1/*n* curve.

To examine the impacts of varying temperature mean and variance on changes in the RBT frequency, we also compute the trends of temperature mean and standard deviation using the nonparametric Theil-Sen method [*Sen*, 1968]. The magnitude of a trend is estimated as the median of trends among all possible data points at a given site. The method is less sensitive to outliers compared to the traditional linear least squares method [*Kumar et al*., 2009]. The statistical trend significance is assessed using the Mann-Kendall test [*Mann*, 1945; *Kendall*, 1975].

4. Observed Record-Breaking Temperatures

To examine the impact of climate change on the RBT frequency in China, we first show trends of annual mean and variance of TX and TN from 1961 to 2013 averaged across China in Figure 1. The station data have been interpolated onto a 1° × 1° latitude-longitude grid using a triangle-based cubic interpolation method [*Barber et al*., 1996] before being area averaged. Note that over grid cells where stations are located, there are only minor differences between the interpolated results averaged over the grid and the original results averaged over available stations. Hence, in order to examine the full picture of RBT characteristics over China, we use the interpolated results over the grid throughout the paper. It is clear that the warming trend (indicated by the dashed line) is relatively larger for TN (at night) than for TX (at day). Both TX and TN increase more in winter than in summer, which is broadly consistent with previous studies [e.g., *Sun et al*., 2013]. Since about

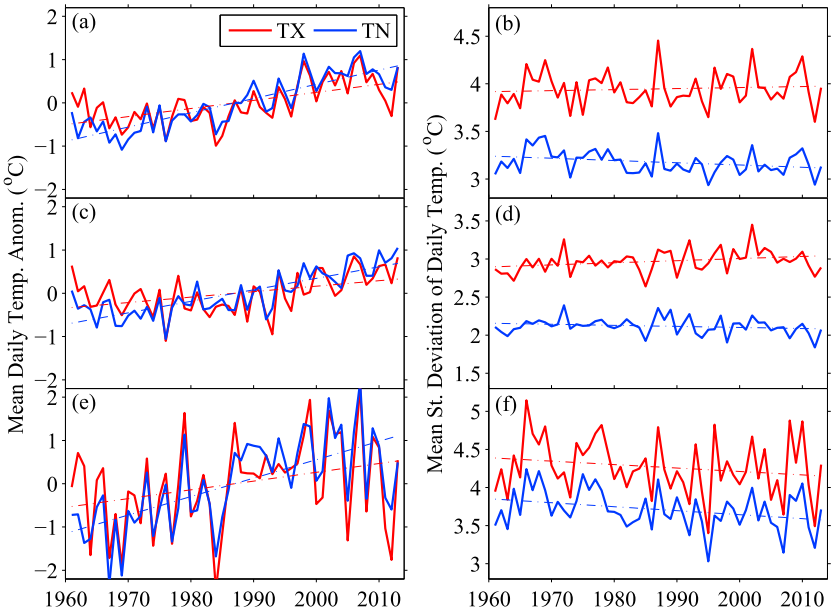

Figure 1. Observed (a, b) annual, (c, d) summer, and (e, f) winter mean daily temperature anomalies (Figures 1a, 1c, and 1e) and standard deviations (Figures 1b, 1d, and 1f) of daily temperatures from 1961 to 2013. The results are area averaged over China. The dashed lines denote the linear trends.

2000, start of the hiatus period with declining global mean temperature [*Jones et al*., 2012], both TX and TN anomalies have experienced a steady decrease but primarily in winter (Figure 1e), implying that a hiatus period is also observed in China but primarily in winter.

To estimate the standard deviation, a linear regression on daily temperatures was first carried out to remove the trend and the mean for each calendar day and for each grid point. The standard deviations of all the grid points were then spatially averaged to obtain the mean standard deviation for each year. The standard deviation calculated from detrended daily temperatures will be used to examine the impact of the short-term variability on changes in RBT hereinafter. The annual trends show that the mean standard deviations of TX remain essentially invariant while those of TN slightly decrease during the period (Figure 1b). In summer, the mean standard deviations slightly increase for TX but are nearly constant for TN. However, after 2000 (i.e., into the hiatus period), the mean standard deviations of both TX and TN have steadily decreased (Figure 1d). The mean standard deviations of both TX and TN in winter continue to decrease during the whole analysis period with large fluctuations (Figure 1f).

4.1. Frequency of Single-Day Record-Breaking Temperatures

Figure 2 shows the decay of observed single-day record highs and lows for TX (left) and TN (right), denoted as HiMax, LoMax, and HiMin, LoMin, respectively, from 1961 to 2013. The results are again area-averaged over the 1°×1° grid in China. The black solid curve represents the theoretical decay rate (1/*n*) as in a stationary climate. It can be seen that only in the early period does the theoretical decay rate fit well to observed records (for both highs and lows). The observed decay rates began to diverge from the theoretical 1/*n* curve since the mid-1990s for TX but since the mid-1980s for TN. It can be also seen that deviations of the observed records from the 1/*n* curve are larger for TN than for TX (Figures 2a and 2b), which is in agreement with previous studies [e.g., *Meehl et al*., 2009; *Pan et al*., 2013a]. These imply that changes in the RBT frequency (relative to a stationary climate) are not only earlier but also larger for TN than for TX during the analysis period.

Taking the linear mean trends into account (represented by the black dashed curves in Figure 2), equation (1) fits the observed annual record highs well before the mid-1990s, after which the fitting falls below the observed records (Figures 2a and 2b), which implies that the warming rate was probably nonlinear during the whole analysis period. Figure S1 in the supporting information shows the same results but using detrended daily temperatures. The decay rates show that the record highs for both TX and TN were below the 1/*n* curve from 1980 to the mid-1990s, after which the record highs increased above the curve

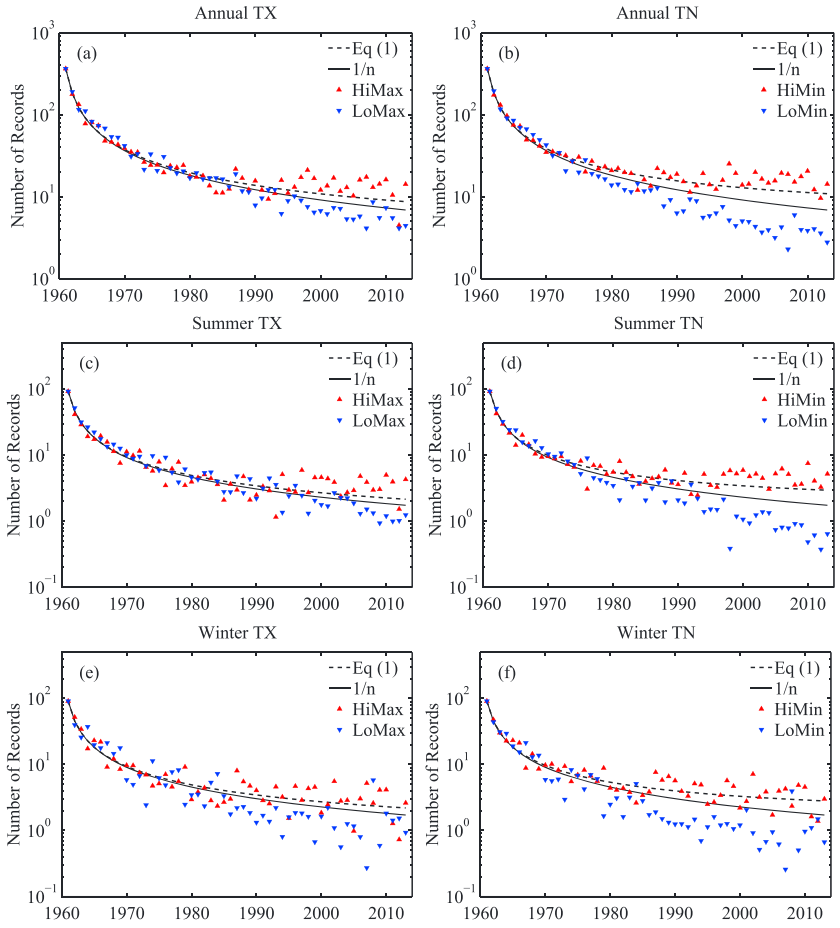

Figure 2. Number of (a, b) annual, (c, d) summer, and (e, f) winter record-breaking high (red triangle) and low (blue triangle) days per year for TX (Figures 2a, 2c, and 2e) and TN (Figures 2b, 2d, and 2f) from 1961 to 2013. The results are area averaged over China. The solid black curve represents the theoretically expected 1/*n* curve, and the dashed black curve is the 1/*n* curve with the linear warming trend term added based on equation (1).

(Figures S1a and S1b). This mid-1990s transition corresponds to the shift of the Atlantic Multidecadal Oscillation (AMO) from cold to warm phase around 1995 [*Wang et al.*, 2013]. However, the impact of nonlinear trends is secondary compared to the linear trend, since the record highs and lows from detrended daily temperatures both slightly fluctuate around the 1/*n* curve, as shown in Figure S1. So from now on, we focus on analyzing the influence of linear trends in this study.

Results shown here can be used to roughly estimate the contribution of the linear mean trend to the increasing frequency of record highs relative to the 1/*n* curve, particularly in recent years when the records clearly deviate from the 1/*n* curve (Figure 2). For example, during the first decade of 21st century (from 2001 to 2010), the observed HiMax and HiMin are 14.1 and 16.7 days per year, respectively, and are 10.0 and 12.5 days per year, respectively, with linear mean TX and TN trends considered. The results should be 8.1 days per year in a stationary climate. As a result, the linear mean trend has increased the frequency of record highs by 32% (=(10.0 − 8.1)/(14.1 − 8.1)) and 51% (=(12.5 − 8.1)/(16.7 − 8.1)) for TX and TN, respectively. This indicates that the impact of the linear mean trend on the RBT frequency is larger for TN than for TX, although we stress here that the trend might be nonlinear. The corresponding percentages in summer (winter) are 25% (36%) and 41% (58%) for TX and TN, respectively, which indicates that the impact of the linear mean trend is larger in winter than in summer.

The annual ratios of single-day record highs to lows for both TX and TN increase from around 1.0 in 1960s to their maxima around the mid-2000s (Figures 3a and 3b), consistent with the annual temperature trends in Figure 1. Since the ratio should be equal to 1 in a stationary climate, deviations from unity can be used as a metric to indicate climate change impact on the RBT frequency. A bootstrap analysis [see *Pan et al.*, 2013a] was performed to

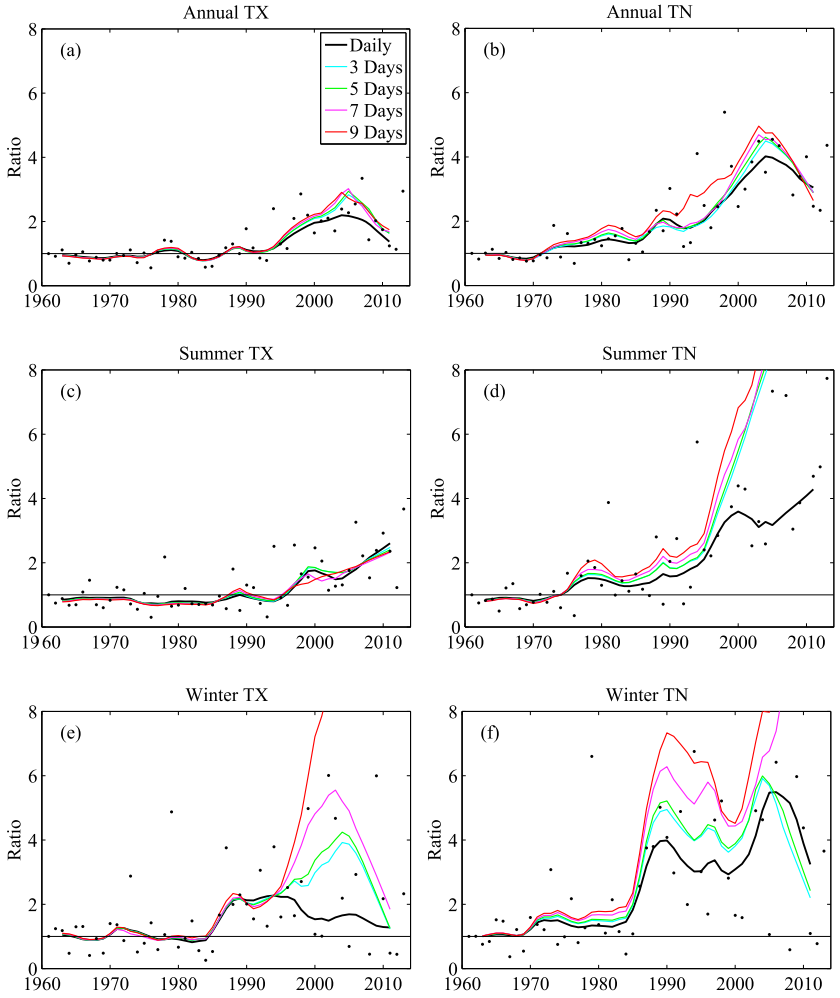

Figure 3. (a, b) Annual, (c, d) summer, and (e, f) winter ratios of single-day record highs to lows (dots) for TX (Figures 3a, 3c, and 3e) and TN (Figures 3b, 3d, and 3f) averaged over China during 1961–2013. The black solid curve is the five-point triple smoothing of the ratios (dots). The colored curves are curve fits to the ratios with a smoothing window (3–9 days). The black horizontal line marks the ratio of 1.

assess the significance of those large ratios in recent years, which suggested that these large values are statistically significant. Note that the results become more spread toward the end. This is because the ratios are obtained with increasingly smaller numerators/denominators (i.e., the record highs and record lows both decrease with time), which is called the heteroscedasticity effect [*Meehl et al.*, 2009].

There are important differences between the ratios for TX and those for TN, as well as the ratios in summer and those in winter. The annual ratios for TX become larger than 1 after about 1990, reaching 2.1 around 2005 and then decreasing afterward (Figure 3a). Nevertheless, the annual ratios for TN become larger than 1 after the mid-1970s and reach 4 around 2005 before starting to decrease (Figure 3b), again indicating that TN has warmed not only earlier but also faster than TX. Table 1 summarizes the ratios for TX and TN during 2001–2010 and the whole analysis period. It can be seen that differences between the ratios for TX and those for TN are larger in summer (2.0 versus 5.4) than in winter (5.1 versus 6.4), indicating that the asymmetry of RBT between TX and TN is larger in summer than in winter. During the hiatus period, the ratios for both TX and TN continue to increase in summer (Figures 3c and 3d), whereas the ratios exhibit a steady negative trend for TX and a wavy behavior for TN in winter (Figures 3e and 3f).

Large regional variability usually exists in the observed RBT frequency [*Coumou et al.*, 2013]. The spatial pattern of single-day ratios for TX averaged over the period 1961–2013 and the corresponding trends of the mean temperatures and variances are displayed in Figure 4. The temporally averaged ratio at each station

Table 1. Single-Day and Multiday Mean Ratios of Record Highs to Lows for TX and TN During 2001–2010 and 1961–2013[a]

	TX			TN		
	Annual	Summer	Winter	Annual	Summer	Winter
Daily	2.1 (1.3)	2.0 (1.3)	5.1 (2.1)	4.0 (2.2)	5.4 (2.8)	6.4 (3.0)
3 days	2.4 (1.4)	2.1 (1.3)	5.8 (2.5)	5.0 (2.4)	6.8 (3.4)	8.6 (4.1)
5 days	2.5 (1.4)	2.2 (1.3)	6.2 (2.6)	5.2 (2.5)	7.0 (3.5)	11.6 (4.5)
7 days	2.7 (1.5)	2.3 (1.3)	7.7 (3.0)	5.7 (2.7)	7.7 (4.0)	16.6 (5.9)
9 days	2.9 (1.6)	2.5 (1.4)	9.1 (3.5)	6.1 (2.9)	8.1 (4.5)	20.7 (7.1)

[a]The results for the latter period are in brackets.

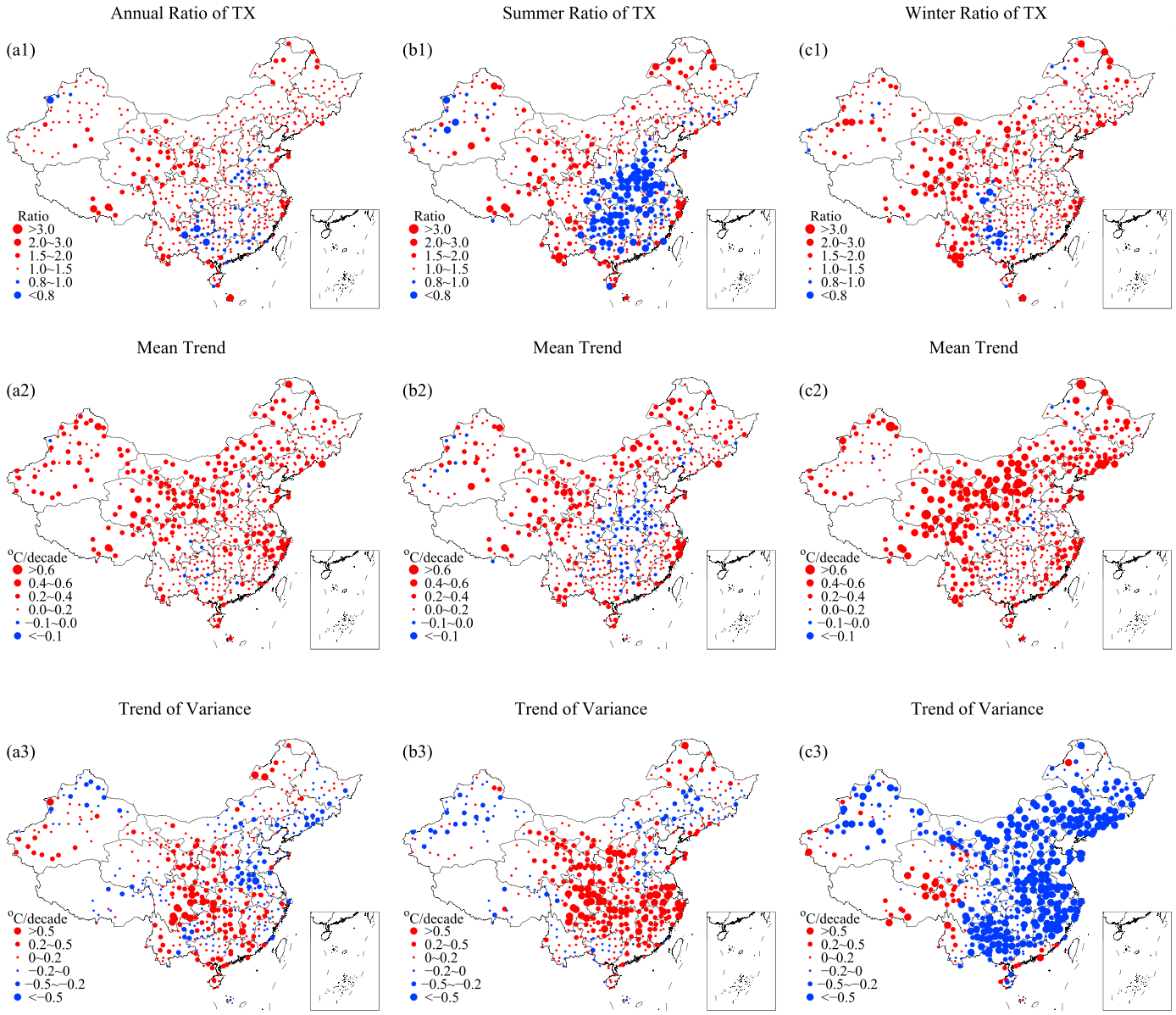

Figure 4. Spatial distributions of (a1–a3) annual, (b1–b3) summer, and (c1–c3) winter ratios averaged over 1961–2013 (Figures 4a1, 4b1, and 4c1), and trends of mean temperatures (Figures 4a2, 4b2, and 4c2), and standard deviations (after detrending, Figures 4a3, 4b3, and 4c3) during 1961–2013 for TX. Only trends significant at the 0.05 significance level are shown. The unit of trends is °C/decade.

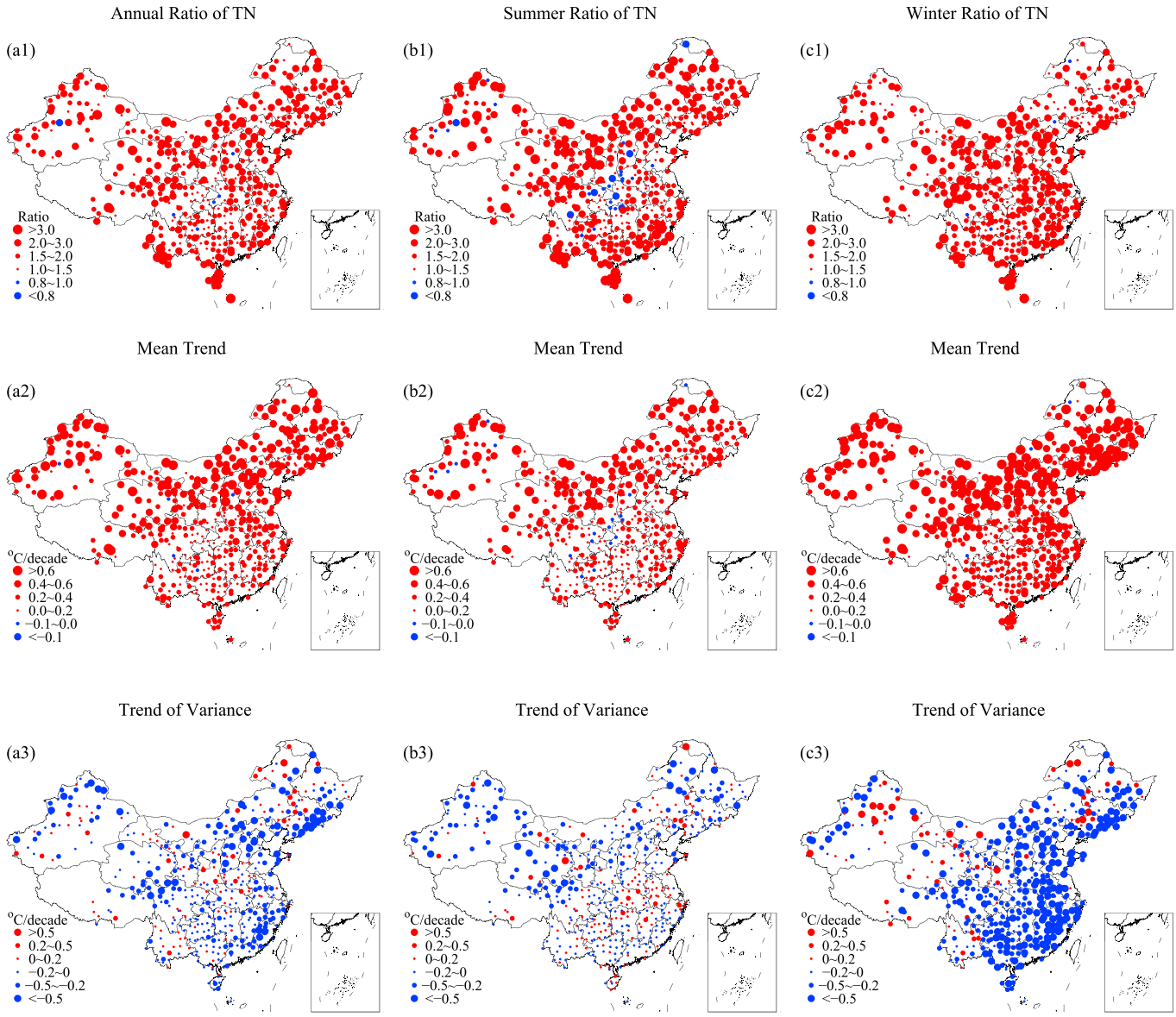

Figure 5. Same as Figure 4, but for TN.

is calculated by averaging the annual records using the number of years *n* as weights, in order to remove the above mentioned heteroscedasticity effect. Figure 4 shows that the annual ratios are larger than 1 over most places with sporadic sites of less than 1 in southern China (Figure 4a1). In summer, the ratios are less than 1 over the central southern China (Figure 4b1), coinciding with the "warming hole" regions that experience cooling in summer [*Pan et al.*, 2004, 2009]. In winter, the ratios are predominantly larger than 1 except for some parts of the southwest (Figure 4c1). The spatial distributions are in broad consistency with previous studies [e.g., *Zhang et al.*, 2011; *Zhou and Ren*, 2011; *Pan et al.*, 2013a]. Changes in the mean temperatures are broadly consistent with changes in the ratios (cf. Figures 4a2 and 4a1), again suggesting important impacts of the linear mean temperature trend on the RBT frequency. Noticeable increases in the temperature variance in summer occur at places where the ratios are less than 1 in the southern China (Figure 4b3), which to some extent explain the low ratios (blue dots in Figure 4b1) with positive linear trends (red dots in Figure 4b2) in some places of the south. As a result, the impact of changes in the temperature variance on the RBT frequency cannot be ignored for summer TX, which corresponds to the relatively low contribution (25%) of the linear mean trend as shown in Figure 2. The temperature variances in winter show negative trends over most of the country except over the southwestern China (near the Tibetan Plateau) and do not appear to be correlated with the pattern of ratios.

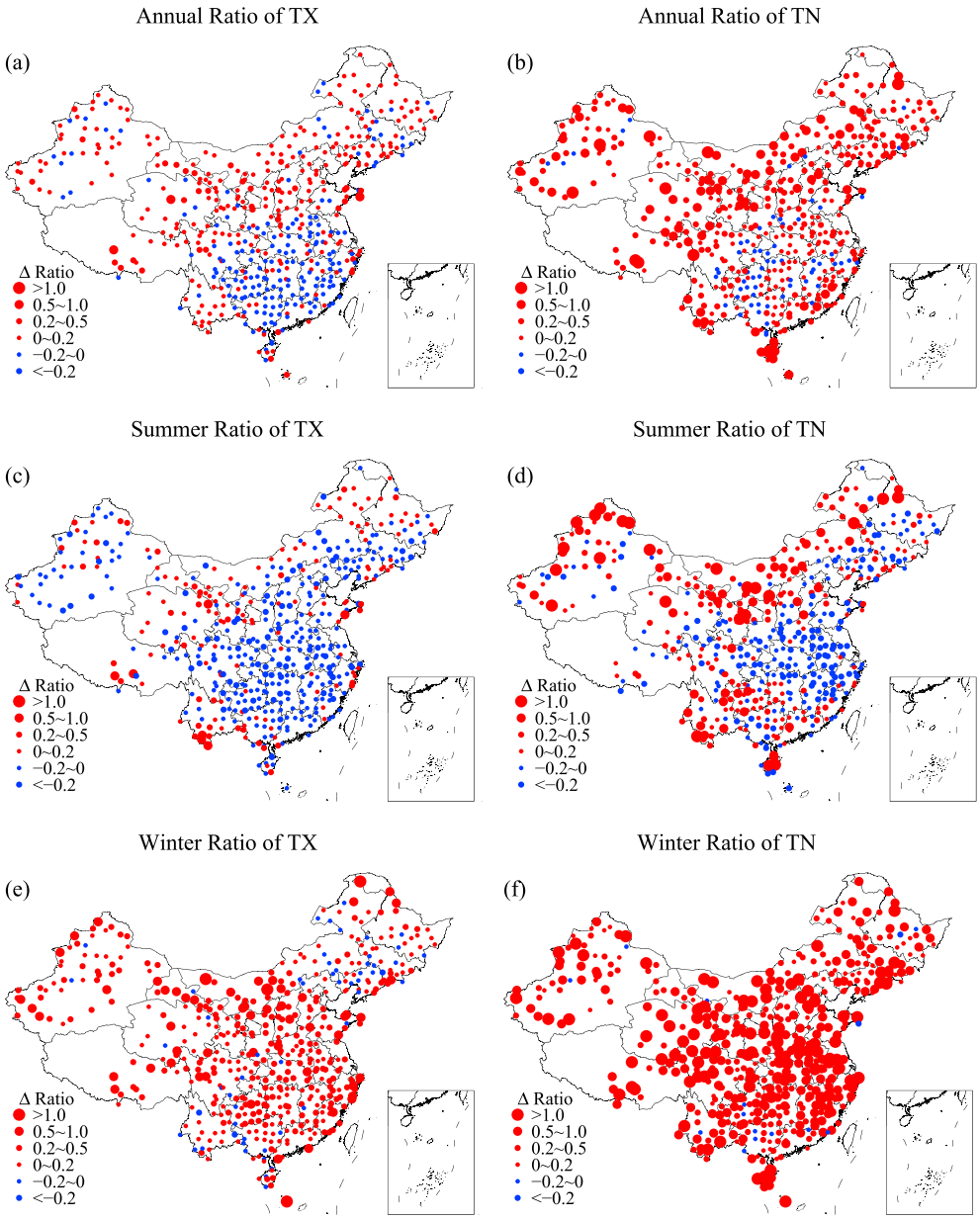

Figure 6. (a, b) Annual, (c, d) summer, and (e, f) winter differences between single-day and 5 day mean ratios of record highs to lows averaged over 1961–2013 for TX (Figures 6a, 6c, and 6e) and TN (Figures 6b, 6d, and 6f). Red dots denote positive values, while blue dots denote negative values.

Figure 5 presents similar results except for TN. As can be seen, the ratios for TN are larger than 1 across the country and are larger than those for TX (cf. Figures 4a1 and 5a1). The pattern of mean trends also agrees well with the pattern of ratios (cf. Figures 5a2 and 5a1). The trends of temperature variance are generally negative over the country, with larger absolute values in winter. These results are all consistent with the spatially averaged results shown in Figure 1.

4.2. Multiday Mean Ratios of Record Highs to Lows

What is also interesting is the ratios of multiday mean record highs to lows since they indicate changes in extreme temperatures averaged over several days like heat waves. To examine multiday mean ratios, we first performed running average on daily temperatures with moving windows of 3, 5, 7, or 9 days. It can be seen from Figure 3 that the multiday mean ratios increase with the lengthening of moving windows, implying that

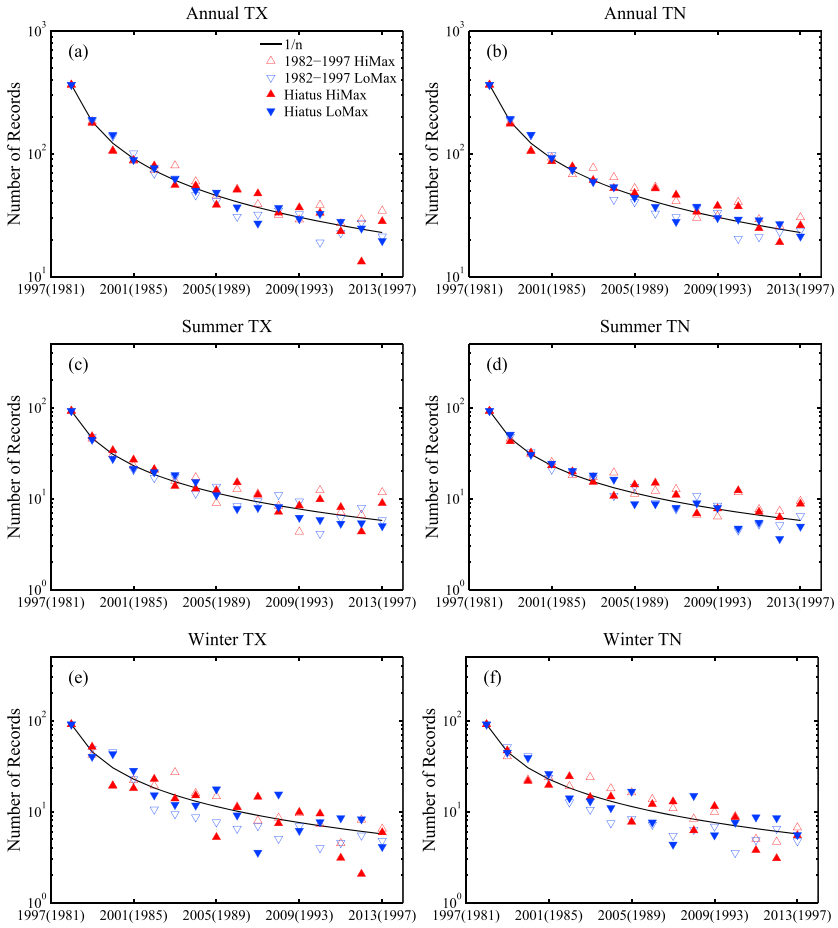

Figure 7. Number of (a, b) annual, (c, d) summer, and (e, f) winter record-breaking high (red triangle) and low (blue triangle) days per year for (Figures 7a, 7c, and 7e) TX and (Figures 7b, 7d, and 7f) TN over China. The solid and hollow triangles indicate the record numbers during the hiatus period and 1982–1997, respectively. The solid black curve represents the 1/*n* curve.

the impact of climate change is stronger on the multiday mean RBTs than on single-day RBTs. This can be explained using equation (1) because the frequency of RBTs increases with the ratio of warming trend to temperature variance, and the temperature variance decreases as the moving window widens [*Rahmstorf and Coumou*, 2011; *Coumou and Rahmstorf*, 2012]. This also explains why the ratios based on monthly records are about 4 over the U.S. [*Wuebbles et al.*, 2014], larger than the ratios based on daily records (about 2) [see *Meehl et al.*, 2009]. At seasonal scales (summer or winter), the ratios increase faster as the moving window expands compared to those at annual scales (Figures 3c–3f). The increases in the ratios are much larger for TN than for TX. Moreover, the increases are larger in winter than in summer (Table 1). These are consistent with larger temperature trends for TN than for TX and larger trends in winter than in summer shown in Figure 1, respectively. Again, this is because equivalent changes in denominators (i.e., temperature variance), but larger numerators (i.e., larger mean temperature trends) result in larger increases in the ratios.

To further examine multiday mean RBTs, Figure 6 shows the spatial distribution of differences between 5 day mean and single-day ratios. The annual 5 day mean ratios for TX are higher in the northern China but lower in the southern China than the single-day ratios, while the ratios for TN are higher across most of the country (Figures 6a and 6b). The higher 5 day mean ratios were roughly equally caused by larger HiMax (HiMin) combined with smaller LoMax (LoMin) (not shown), that is, the multiday mean HiMax occurs more frequently than the single-day counterpart over northern China, while the multiday mean LoMin is less frequent over most parts of China, and vice versa for multiday mean LoMax and HiMin. When the summer and winter seasons are separated, it is clear that the 5 day mean ratios in summer are smaller than the single-day counterparts

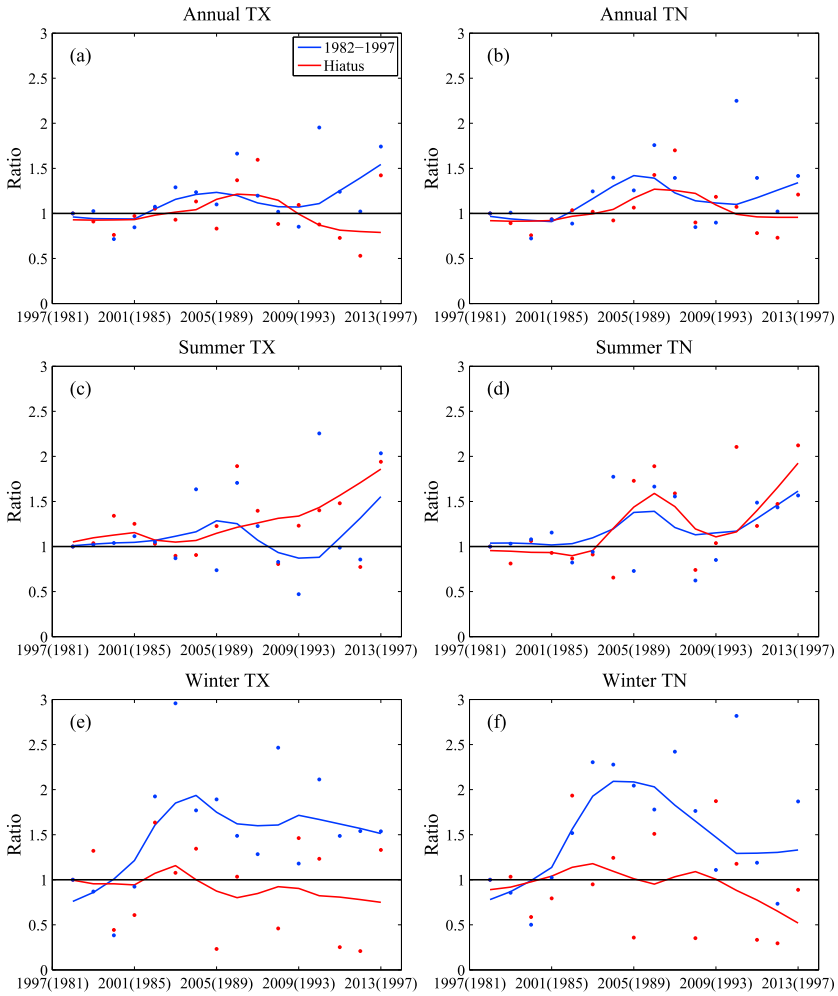

Figure 8. (a, b) Annual, (c, d) summer, and (e, f) winter ratios of single-day record highs to lows for TX (Figures 8a, 8c, and 8e) and TN (Figures 8b, 8d, and 8f). The red and blue solid curves are the smoothed curve fits during the hiatus period (red dots) and 1982–1997 (blue dots), respectively. The black horizontal line marks the ratio of 1.

over most places for TX while only over the central China for TN (Figures 6c and 6d). Whereas the 5 day mean ratios in winter are overwhelmingly larger than the single-day ratios across China, with bigger differences for TN than for TX (Figures 6e and 6f).

Note that the 3 day and 5 day mean ratios have different trends from the 7 day and 9 day ratios over the last decade, especially in winter (Figure 3). To examine if the conclusions drawn from 5 day mean ratios in Figure 6 would hold for other multiday scales, we repeated the analysis for 3 day (Figure S2) and 7 day (Figure S3) mean ratios. The results show that the patterns of differences for 3 day and 7 day mean ratios are consistent with the pattern of differences for 5 day results. Thus, it can be concluded that the finding above applies for multiday (from 3 to 9 days) mean ratios in general.

4.3. Record-Breaking Temperature Frequency in the Hiatus Period

According to Figure 3, changes in the single-day ratios continue to increase in summer but decrease in winter during the hiatus period. To assess changes in the RBT frequency during global warming in comparison to the hiatus period, we computed the number of single-day RBT during 1982–1997 and 1998–2013, respectively. The former is a period when climate warming is relatively strong. The results are shown in Figure 7. It is clear that in summer, the number of LoMax/LoMin in most years during the hiatus period was less than their counterparts in 1982–1997, while only in a few years the number of HiMax/HiMin during the hiatus period was larger (Figures 7c and 7d). In winter, most record high (low) numbers during the hiatus period are less (more) than those in 1982–1997 (Figures 7e and 7f).

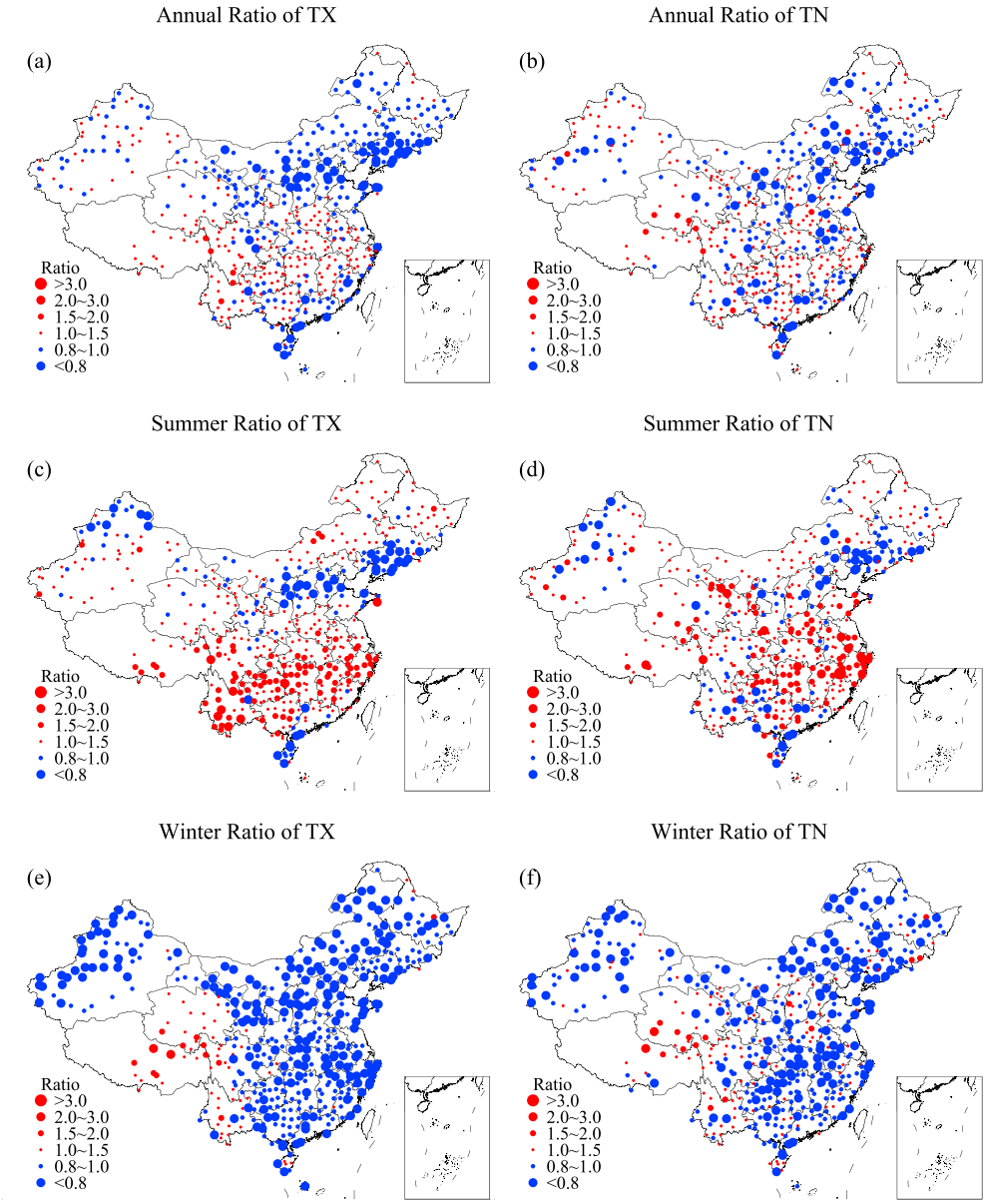

Figure 9. (a, b) Annual, (c, d) summer, and (e, f) winter ratios of record highs to lows averaged over the hiatus period for TX (Figures 9a, 9c, and 9e) and TN (Figures 9b, 9d, and 9f). Red dots denote ratios that are larger than 1, while blue dots denote ratios that are smaller than 1.

Figure 8 shows that the corresponding ratios in the hiatus period and during 1982–1997. As can be seen, the annual ratios are generally lower in the hiatus period for both TX and TN (Figures 8a and 8b). In summer, mean temperatures of both TX and TN continue to increase in the hiatus period, with a higher rate than that during 1982–1997 (Figure 1c). As a result, the ratios in the hiatus period are generally larger than their counterparts during 1982–1997 (Figures 8c and 8d), which is primarily due to the lower number of record lows (Figures 7c and 7d). The variances of both TX and TN experience a steady decrease after 2000 (Figure 1d), indicating that the width of the temperature distribution reduces while the distribution shifts to a warming regime. Given that record highs (lows) depend on the right (left) tail of the distribution, the reduced width enhances the rightward shifting of the left tail and offsets the rightward shift of the right tail, making it more difficult for both record lows and highs to occur as compared to the case where the width remains unchanged. This explains why record lows are less in general and why only a few record highs are larger in the hiatus period as compared to their counterparts during 1982–1997. Again, it implies that the

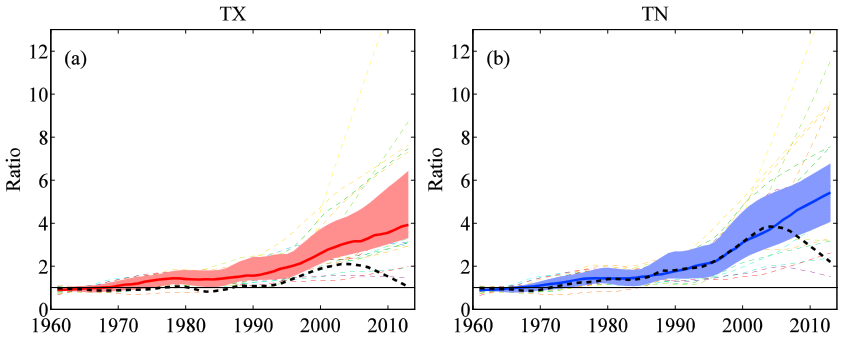

Figure 10. Ratios of record highs to lows computed from CMIP5 models using historical and RCP8.5 experiments for (a) TX and (b) TN during 1961–2013. The thick solid lines are multimodel median, and the dashed black lines are observed values. Shading indicates the multimodel interquartile (25–75%) range. Dashed thin lines indicate individual model simulations.

impact of varying temperature variance is also important in summer. In winter, the ratios are clearly less in the hiatus period than during 1982–1997 (Figures 8e and 8f). The winter ratios in the hiatus period are more or less constant in the first few years and then decrease to less than 1, which mainly reflects the winter cooling during the hiatus period.

Figure 9 shows the patterns of temporally averaged single-day ratios for TX and TN during the hiatus period. The temporally averaged ratio at each station was again computed with weights 1/*n*. As can be seen, all the spatial distributions are almost anticorrelated to those for the entire analysis period (Figures 4a1–4c1 and 5a1–5c1). Annual ratios for TX are less than 1 in the northern and far southern China, while larger than 1 in the central China. Annual ratios for TN are relatively cluttered (Figures 9a and 9b). The summer ratios are evidentially larger than 1 over southern China, while the winter ratios are less than 1 across most of the country (Figures 9c–9f). As a result, it can be concluded that the larger ratios in summer during the hiatus period seen in Figure 8 primarily come from the southern China, while the smaller ratios in winter occur across most of the country.

5. Simulated Record-Breaking Temperatures in CMIP5 Models

Simulations from 28 CMIP5 models are analyzed in this section to assess the models' capability in capturing RBT characteristics and possible future changes in the RBT frequency. Here one single *historical* or RCP8.5 ensemble member for each model is presented (see section 2), totaling 28 members. The ensembles are *r1i1p1* except for ACCESS1-3 (*historical r2i1p1*), GISS-E2-H (*historical r6i1p1*, RCP8.5 *r2i1p3*), GISS-E2-R (*historical r6i1p1*, RCP8.5 *r2i1p1*), IPSL-CM5A-MR (*historical r2i1p1*), and MPI-ESM-LR (RCP8.5 *r3i1p1*).

5.1. Twentieth Century

First, the simulated single-day record ratios in CMIP5 simulations are validated. Figure 10 shows the spatially averaged annual ratios over China from 28 CMIP5 models during 1961–2013. Model data from historical and RCP8.5 runs were used for 1961–2005 and 2006–2013 period, respectively. There is appreciable intermodel variability, indicated by the dashed thin lines for individual models and the shading for interquartile ranges. To evaluate the models' performance, the observed ratios, indicated by the thick black dashed line, are also shown for the comparison. Before around 2005, the multimodel median of the ratios, indicated by the thick solid curve, generally captures the trends of both TX and TN such as the cooling in the first half of 1980s and the rapid increase after 1990. Simulations also capture well the magnitude of the single-day ratios for TN; however, simulations significantly overestimate the magnitude of single-day ratios for TX, resulting in a much smaller asymmetry between TX and TN as compared to observations. During the hiatus period, models fail to reproduce the decreasing trends of annual ratios for both TX and TN in recent years (after around 2005) since the simulated ratios keep increasing.

The larger model biases for TX ratios are likely associated with the presence of warming hole in the central southern China, particularly in summer. Most CMIP5 models fail to simulate or underestimate the relative cooling in the warming hole region [*Pan et al.*, 2013b]. To verify whether the overestimation of the ratio for TX is associated with underestimating the cooling in the warming hole region, Figure 11 shows the

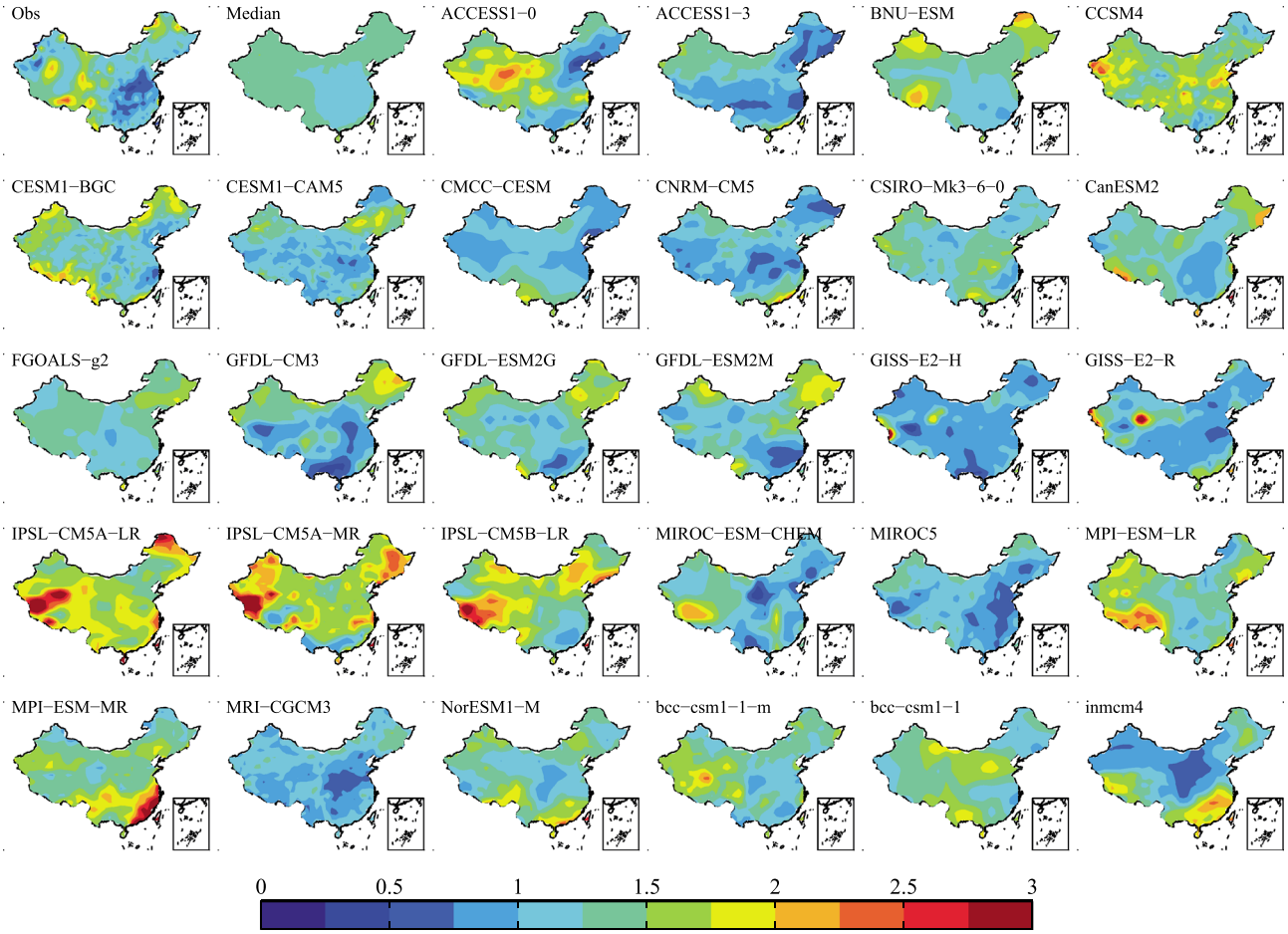

Figure 11. (first row) Observed and simulated summer ratios of record highs to lows for TX averaged over 1961–2005. (second row) The multimodel median is shown, and (third to fifth rows) the others are from the 28 individual models listed in Table S1.

performances of individual models for the single-day summer ratios for TX over the period 1961–2005. The temporally averaged ratios are calculated in the same way as in Figure 4. The pattern is chosen for two reasons. First, the decrease of TX over the warming hole mainly occurs in summer [*Pan et al*., 2004, 2009]. Second, summer hot extremes typically have significant socioeconomic consequences [e.g., *Anderson and Bell*, 2011; *Li and Bou-Zeid*, 2013]. Models show a wide diversity in the simulated ratios over China. Compared to the observations plotted as in Figure 11 (first panel, first row) based on the interpolated values, some models reproduce well the locations of low-value regions (i.e., the warming hole regions) but overestimate the magnitude, while some models reproduce the magnitude but at the wrong locations. For example, CanESM2 produces a pattern similar to the observed one but overestimates the low values. In a separate study, CanESM2 was found to be good at simulating the cooling trend in the warming hole region in the central U.S. [*Pan et al*., 2013b]. On the other hand, ACCESS1 (0 and 3) and Geophysical Fluid Dynamics Laboratory (CM3, ESM2G, and ESM2M) models capture the magnitude of the low-value ratios, but the locations are slightly biased. Other models, such as IPSL-CM5A (LR and MR), hardly reproduce the observed low-value regions since they significantly overestimate the ratios across most of China. The multimodel median (Figure 11, second panel, first row) overestimates the low-value ratios in the central southern China while underestimates the high-value ratios in some parts of the western and northeastern China. It should be pointed out that the underestimation of ratios in the west by models is partly due to the interpolation error given to the very sparse station coverage. Thus, it can be concluded that model simulations generally overestimate the ratios for TX due to the failure of capturing the cooling in the warming hole region, and the multimodel median shows a more uniform warming than observations, in agreement with a previous study in the U.S. by *Meehl et al*. [2009].

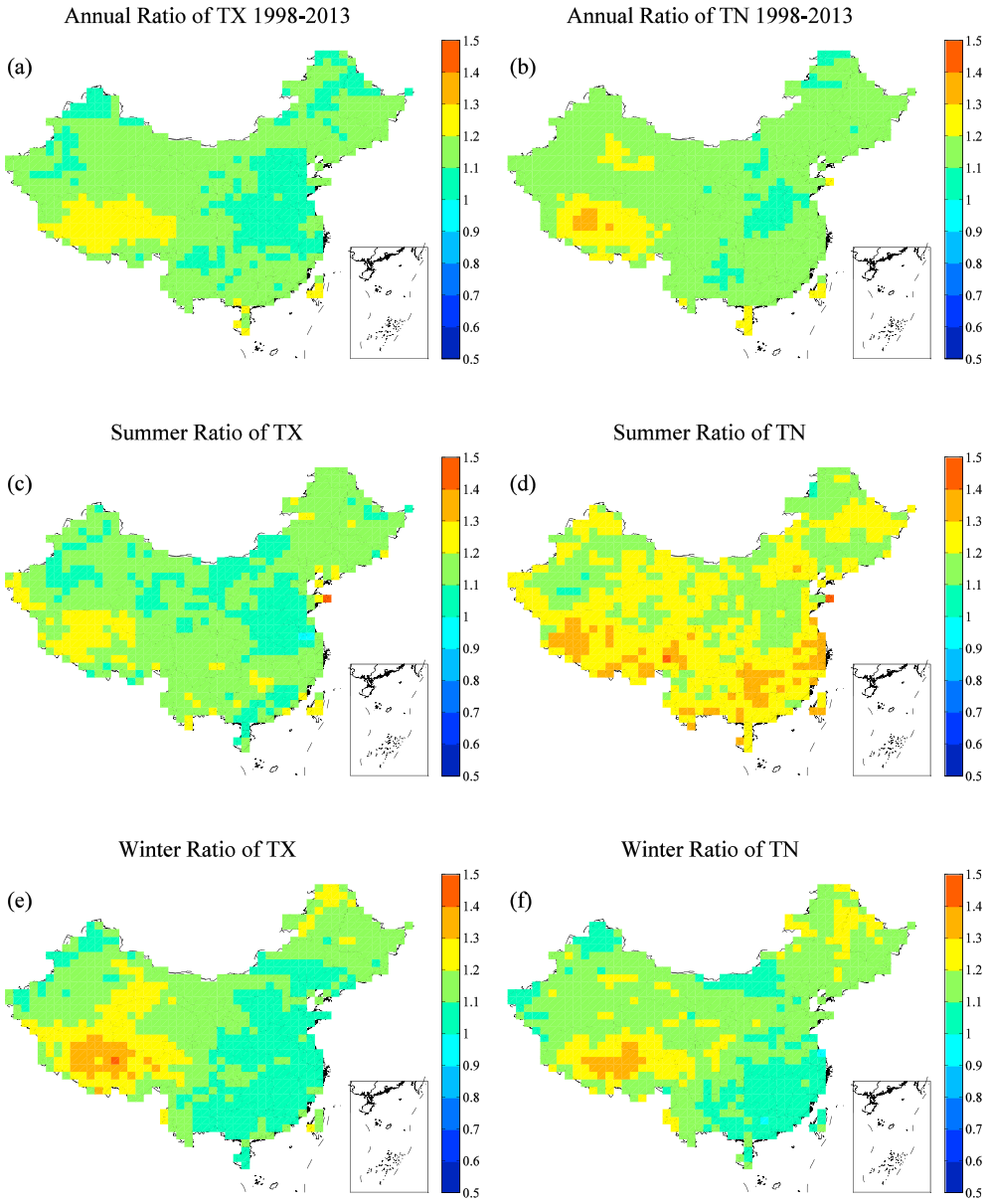

Figure 12. (a, b) Annual, (c, d) summer, and (e, f) winter ratios of record highs to lows from CMIP5 model simulations during the hiatus period for TX (Figures 12a, 12c, and 12e) and TN (Figures 12b, 12d, and 12f). The results are the median of 28 model simulations listed in Table S1.

To further examine the models' performance on simulating the RBT frequency during the hiatus period, Figure 12 shows the temporally averaged single-day ratios over the hiatus period (1998–2013). As can be seen, the simulated patterns from multimodel medians show less spatial variability as compared to the observations in Figure 9. The simulated ratios for both TX and TN are larger than 1 over the whole country, with some large values in the Tibet Plateau. In summer, the simulations for TN reproduce the large ratios in southwestern China, but with smaller magnitudes than the observations (cf. Figures 12d and 9d). The simulated ratios in winter are generally less than those in summer for both TX and TN (Figures 12e and 12f), which is consistent with the observations. However, models do not reproduce well the ratios less than 1 in the observations. In summary, it can be concluded that the RBT characteristics during the hiatus period is not reasonably reproduced by CMIP5 models, which agrees with other previous studies based on model data from historical and RCP4.5 runs [*Kamae et al.*, 2014; *Sillmann et al.*, 2014].

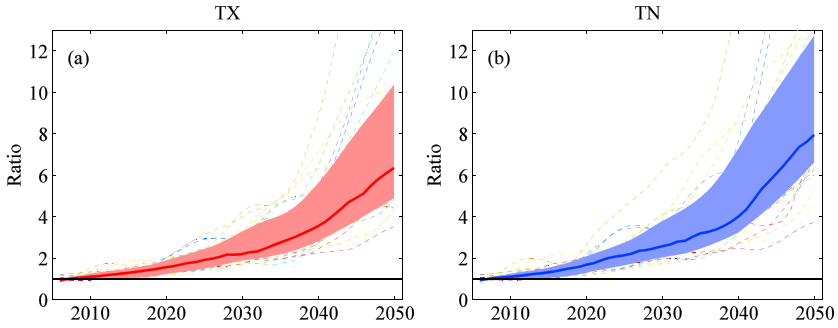

Figure 13. Ratios of record highs to lows computed from CMIP5 models using RCP8.5 experiments for (a) TX and (b) TN during 2006–2050. The thick solid lines are multimodel median. Shading indicates the multimodel interquartile (25–75%) range. Dashed thin lines indicate individual model simulations.

5.2. Twenty-First Century

Projections of the ratios in the RCP8.5 scenario are presented over the period 2006–2050 (Figure 13). However, it is important to keep in mind that the simulations examined in our study have already shown some significant biases, which are unlikely to disappear in future runs. It can be seen from Figure 13 that as the climate continues to warm, the ratios increase at a faster rate than in historical runs. By the end of the period, the ratios reach 6 for TX and 8 for TN, which are about twice the values at the end of historical runs (i.e., 2005). Note that the increasing rates accelerate after about 2040 for both TX and TN ratios, which is likely due to the accelerated increase of the greenhouse gas forcing in the RCP8.5 scenario [*Moss et al.*, 2010]. The asymmetry of ratios between TX and TN in the projection, similar to that in the historical run, is smaller than that in the observation, which implies that the model uncertainty is largely attributed to model intrinsic systematic biases and these biases will likely persist in the projection. That is, the overestimation of ratios for TX likely persists in both historical and future simulations. Moreover, it can be seen that the intermodel uncertainty in future projections is more significant than that in historical experiments, reflected by the wider shading area. However, although the projections are to a certain extent model dependent [*Meehl et al.*, 2009], all simulations show general increases in the ratios in the RCP8.5 scenario.

6. Summary and Discussions

We have evaluated both the observed and model-simulated RBT in China based on up-to-date daily maximum and minimum surface air temperature measurements from 532 stations and 28 CMIP5 model simulations. The impact of warming trend on changes in the RBT frequency is examined, with a specific focus on RBT characteristics during the hiatus period. Also, CMIP5 models' skill in reproducing the observed RBT frequency is assessed and future changes in RBT in RCP8.5 experiments are also examined. Based on these analyses, the following main conclusions are drawn:

1. Changes in the RBT frequency occurred not only earlier but also faster for TN than for TX during the last five decades. The ratio of single-day record high to low exceeded 1 only after about 1990 for TX, but as early as the mid-1970s for TN, and reached 2.1 and 4.0 during the first decade of 21st century for TX and TN, respectively. The asymmetry of the RBT frequency between TX and TN in summer is larger than in winter. Changes in the RBT frequency are largely associated with the mean temperature trend, especially in winter, and to a lesser extent associated with changes in temperature variance in summer. The impact of the linear mean trend on the RBT frequency is more significant for TN than for TX.
2. The ratios are larger for multiday moving-averaged temperatures than for daily temperatures, indicating that the impact of climate change is more significant for multiday mean RBTs than for single-day RBTs. Compared to the single-day ratios, the multiday mean ratios are larger in the northern China but smaller in the southern China for TX, while larger over most of the country for TN. Moreover, only in summer are the multiday mean ratios less than the single-day ratios in some places, whereas in winter the multiday mean ratios are overwhelmingly larger.
3. In the hiatus period (1998–2013), the ratios for both TX and TN continue to increase in summer but decrease in winter, which are broadly consistent with the trends of seasonal mean temperatures.

Compared to the ratios in the period 1982–1997, the summer ratios in the hiatus period were generally higher primarily due to fewer record lows, since the decreasing temperature variance suppressed the increase in record highs. The winter ratios in the hiatus period were much less than their counterparts in 1982–1997 and decreased to less than 1 due to the winter cooling. The summer increases occurred mainly in southern China, whereas the winter decreases were across most of the country.

4. Model simulations in China show a much smaller asymmetry between TX and TN in terms of the RBT frequency as compared to the observations. The multimodel median reproduces well the single-day ratios for TN but overestimates the ratios for TX, which is largely because most models fail to capture the relative cooling in the warming hole area. Most CMIP5 models cannot reproduce the observed decreases in ratios during the hiatus period but rather show a more uniform pattern with values larger than 1.
5. The ratios of record highs to lows projected under the high-emission RCP8.5 scenario continue to increase during 2006–2050. The increasing rates for both TX and TN are about twice as those in historical runs, and increases will accelerate after 2040. However, future projections are model dependent with significant intermodel uncertainty, especially for TN.

This study also provides preliminary evaluation of the performance of CMIP5 models in terms of RBT characteristics in historical simulations. The results show that CMIP5 models largely do not capture the asymmetry between TX and TN and the RBT characteristics in the hiatus period. It should be noted that the results shown here are from ocean-atmosphere coupled models, where the decadal variability of sea surface temperatures such as AMO may be different among models [*Pan et al*., 2013b]. As such, multimodel medians may not represent model consensus due to the partial cancelations among models with different phases of AMO. Future work needs to separate models based on the phases of decadal oscillations of sea surface temperatures as *Kumar et al*. [2013] and *Pan et al*. [2013b].

Acknowledgments

This study is supported by the National Natural Science Foundation of China under grants 41475085 and 41275022, the National Program on Key Basic Research Project of China (973) under grant 2012CB417203, the International S&T Cooperation Program of China (ISTCP) under grant 2011DFG23210, and Graduate Education Innovation Project of Jiangsu Province KYLX_0849. We acknowledge the modeling groups, the Program for Climate Model Diagnosis and Intercomparison (PCMDI), and the WCRP's Working Group on Coupled Modeling (WGCM) for their roles in making available the WCRP CMIP5 multimodel data set (http://pcmdi9.llnl.gov/esgf-web-fe/). The observed temperatures were obtained from National Meteorological Information Center of China Meteorological Administration (http://cdc.cma.gov.cn/home.do). We are grateful to three anonymous reviewers for their careful review and valuable comments, which led to a substantial improvement of this manuscript.

References

Anderson, G. B., and M. L. Bell (2011), Heat waves in the United States: Mortality risk during heat waves and effect modification by heat wave characteristics in 43 U.S. communities, *Environ. Health Perspect.*, *119*, 210–218.

Arnold, B. C., N. Balakrishnan, and H. N. Nagaraja (1998), *Records*, 312 pp., John Wiley, New York.

Barber, C. B., D. P. Dobkin, and H. T. Huhdanpaa (1996), The quickhull algorithm for convex hulls, *ACM Trans. Math. Software*, *22*(4), 469–483.

Coumou, D., and S. Rahmstorf (2012), A decade of weather extremes, *Nat. Clim. Change*, *2*, 491–496, doi:10.1038/NCLIMATE1452.

Coumou, D., A. Robinson, and S. Rahmstorf (2013), Global increase in record-breaking monthly-mean temperatures, *Clim. Change*, *118*, 771–782.

Curry, J. (2014), Uncertain temperature trend, *Nat. Geosci.*, *7*, 83–84.

Donat, M. G., and L. V. Alexander (2012), The shifting probability distribution of global daytime and night-time temperatures, *Geophys. Res. Lett.*, *39*, L14707, doi:10.1029/2012GL052459.

Fyfe, J. C., N. P. Gillett, and F. W. Zwiers (2013), Overestimated global warming over the past 20 years, *Nat. Clim. Change*, *3*, 767–769.

Hansen, J., R. Ruedy, M. Sato, and K. Lo (2010), Global surface temperature change, *Rev. Geophys.*, *48*, RG4004, doi:10.1029/2010RG000345.

Hansen, J., M. Sato, and R. Ruedy (2012), Perception of climate change, *Proc. Natl. Acad. Sci. U.S.A.*, *109*, E2415–E2423.

Ji, F., et al. (2014), Evolution of land surface air temperature trend, *Nat. Clim. Change*, *4*, 462–466, doi:10.1038/nclimate2223.

Jones, P. D., D. H. Lister, T. J. Osborn, C. Harpham, M. Salmon, and C. P. Morice (2012), Hemispheric and large-scale land-surface air temperature variations: An extensive revision and an update to 2010, *J. Geophys. Res.*, *117*, D05127, doi:10.1029/2011JD017139.

Kamae, Y., H. Shiogama, M. Watanabe, and M. Kimoto (2014), Attributing the increase in Northern Hemisphere hot summers since the late 20th century, *Geophys. Res. Lett.*, *41*, 5192–5199, doi:10.1002/2014GL061062.

Kendall, M. G. (1975), *Rank Correlation Methods*, Charles Griffin, London.

Kharin, V. V., F. W. Zwiers, X. Zhang, and M. Wehner (2013), Changes in temperature and precipitation extremes in the CMIP5 ensemble, *Clim. Change*, *119*, 345–357.

Kumar, S., V. Merwade, J. Kam, and K. Thurner (2009), Stream flow trends in Indiana: Effects of long term persistence, precipitation and subsurface drains, *J. Hydrol.*, *374*, 171–183.

Kumar, S., J. Kinter III, P. A. Dirmeyer, Z. Pan, and J. Adams (2013), Multidecadal climate variability and the "warming hole" in North America: Results from CMIP5 twentieth- and twenty-first-century climate simulations, *J. Clim.*, *26*, 3511–3527.

Li, D., and E. Bou-Zeid (2013), synergistic interactions between urban heat islands and heat waves: The impact in cities is larger than the sum of its parts, *J. Appl. Meteorol. Climatol.*, *52*, 2051–2064.

Li, Q., H. Zhang, J. Chen, W. Li, X. Liu, and P. D. Jones (2009), A mainland China homogenized historical temperature dataset of 1951–2004, *Bull. Am. Meteorol. Soc.*, *90*, 1062–1065.

Mann, H. B. (1945), Nonparametric tests against trend, *Econometrica*, *13*, 245–259.

Meehl, G. A., C. Tebaldi, G. Walton, D. Easterling, and L. McDaniel (2009), Relative increase of record high maximum temperatures compared to record low minimum temperatures in the U.S, *Geophys. Res. Lett.*, *36*, L23701, doi:10.1029/2009GL040736.

Meehl, G. A., J. M. Arblaster, J. Y. Fasullo, A. Hu, and K. E. Trenberth (2011), Model-based evidence of deep-ocean heat uptake during surface-temperature hiatus periods, *Nat. Clim. Change*, *1*, 360–364.

Meehl, G. A., A. Hu, J. M. Arblaster, J. Y. Fasullo, and K. E. Trenberth (2013), Externally forced and internally generated decadal climate variability associated with the Interdecadal Pacific Oscillation, *J. Clim.*, *26*, 7298–7310.

Moss, R. H., et al. (2010), The next generation of scenarios for climate change research and assessment, *Nature*, *463*, 747–756, doi:10.1038/nature08823.

Pan, Z., R. W. Arritt, E. S. Takle, W. J. Gutowski Jr., C. J. Anderson, and M. Segal (2004), Altered hydrologic feedback in a warming climate introduces a "warming hole", *Geophys. Res. Lett.*, *31*, L17109, doi:10.1029/2004GL02528.

Pan, Z., M. Segal, X.-Z. Li, and B. Zib (2009), Global climate change impact on the Midwestern U.S.—A summer cooling trend, in *Climate Variability, Predictability, and Change in the Midwestern United States*, edited by S. Pryor, pp. 29–41, Indiana Univ. Press, Indianapolis.

Pan, Z., B. Wan, and Z. Gao (2013a), Asymmetric and heterogeneous frequency of high and low record-breaking temperatures in China as an indication of warming climate becoming more extreme, *J. Geophys. Res. Atmos.*, *118*, 6152–6164, doi:10.1002/jgrd.50467.

Pan, Z., X. Liu, S. Kumar, Z. Gao, and J. Kinter (2013b), Intermodel variability and mechanism attribution of central and southeastern U.S. anomalous cooling in the twentieth century as simulated by CMIP5 models, *J. Clim.*, *26*, doi:10.1175/JCLI-D-12-00559.1.

Rahmstorf, S., and D. Coumou (2011), Increase of extreme events in a warming world, *Proc. Natl. Acad. Sci. U.S.A.*, *108*, 17,905–17,909, doi:10.1073/pnas.1101766108.

Ren, G. Y., Y. H. Ding, Z. C. Zhao, J. Y. Zheng, T. W. Wu, G. L. Tang, and Y. Xu (2012), Recent progress in studies of climate change in China, *Adv. Atmos. Sci.*, *29*(5), 958–977, doi:10.1007/s00376-012-1200-2.

Schär, C., P. L. Vidale, D. Lüthi, C. Frei, C. Häberli, M. Liniger, and C. Appenzeller (2004), The role of increasing temperature variability in European summer heatwaves, *Nature*, *427*, 332–336.

Sen, P. K. (1968), Estimates of the regression coefficients based on Kendall's tau, *J. Am. Stat. Assoc.*, *63*, 1379–1389.

Seneviratne, S. I., M. G. Donat, B. Mueller, and L. V. Alexander (2014), No pause in the increase of hot temperature extremes, *Nat. Clim. Change*, *4*, 161–163.

Sillmann, J., M. G. Donat, J. C. Fyfe, and F. W. Zwiers (2014), Observed and simulated temperature extremes during the recent warming hiatus, *Environ. Res. Lett.*, *9*, doi:10.1088/1748-9326/9/6/064023.

Simolo, C., M. Brunetti, M. Maugeri, and T. Nanni (2011), Evolution of extreme temperatures in a warming climate, *Geophys. Res. Lett.*, *38*, L16701, doi:10.1029/2011GL048437.

Sun, L.-D., C.-J. Zhang, H.-Y. Zhao, J.-J. Lin, and W. Qu (2013), Features of climate change in Northwest China during 1961–2010, *Adv. Clim. Change Res.*, *4*(1), doi:10.3724/SP.J.1248.2013.012.

Sun, Y., X. Zhang, F. W. Zwiers, L. Song, H. Wan, T. Hu, H. Yin, and G. Ren (2014), Rapid increase in the risk of extreme summer heat in Eastern China, *Nat. Clim. Change*, *4*, 1082–1085, doi:10.1038/NCLIMATE2410.

Taylor, K. E., R. J. Stouffer, and G. A. Meehl (2012), An overview of CMIP5 and the experiment design, *Bull. Am. Meteorol. Soc.*, *93*, 485–498, doi:10.1175/BAMS-D-11-00094.1.

Trewin, B., and H. Vermont (2010), Changes in the frequency of record temperatures in Australia, 1957–2009, *Aust. Meteorol. Oceanog. J.*, *60*, 113–119.

Wang, J. L., B. Yang, F. C. Ljungqvist, and Y. Zhao (2013), The relationship between the Atlantic Multidecadal Oscillation and temperature variability in China during the last millennium, *J. Quat. Sci.*, *28*(7), 653–658.

Wang, X. L., Q. H. Wen, and Y. Wu (2007), Penalized maximal t test for detecting undocumented mean change in climate data series, *J. Appl. Meteorol. Climatol.*, *46*, 916–931.

Wen, Q. H., X. Zhang, Y. Xu, and B. Wang (2013), Detecting human influence on extreme temperatures in China, *Geophys. Res. Lett.*, *40*, 1171–1176, doi:10.1002/grl.50285.

Wergen, Q., and J. Krug (2010), Record-breaking temperatures reveal a warming climate, *Europhys. Lett.*, *92*(3), doi:10.1209/0295-5075/92/30008.

Wuebbles, D., et al. (2014), CMIP5 climate model analyses climate extremes in the United States, *Bull. Am. Meteorol. Soc.*, *95*(4), 571–583.

Xiong, K.-G., G.-L. Feng, Q.-G. Wang, and J.-G. Hu (2009), Spatialtemporal characteristics of record-breaking temperature events over China in recent 46 years [in Chinese], *Acta Phys. Sin.*, *58*, 8107–8115.

You, Q., S. Kang, E. Aguilar, and Y. Yan (2011), Changes in daily climate extremes in China and their connection to the large scale atmospheric circulation during 1961–2003, *Clim. Dyn.*, *36*, 2399–2417, doi:10.1007/s00382-009-0735-0.

Zhai, P., X. Zhang, H. Wan, and X. Pan (2005), Trends in total precipitation and frequency of daily precipitation extremes over China, *J. Clim.*, *18*, 1096–1108.

Zhang, D.-Q., J. Yang, Q.-G. Wang, and G.-L. Feng (2009), Analysis of climate record breaking temperature events in China during the past 50 years [in Chinese], *Acta Phys. Sin.*, *58*, 4354–4362.

Zhang, Q., J. F. Li, Y. D. Chen, and X. H. Chen (2011), Observed changes of temperature extremes during 1960–2005 in China: Natural or human induced variations?, *Theor. Appl. Climatol.*, *106*, 417–431.

Zhou, T. J., S. Ma, and L. Zou (2014), Understanding a hot summer in central eastern China: Summer 2013 in context of multimodel trend analysis, in S. C. Herring, M. P. Hoerling, T. C. Peterson, and P. A. Stott (2014), explaining extreme events of 2013 from a climate perspective, *Bull. Am. Meteorol. Soc.*, *95*(9), S54–S57.

Zhou, Y. Q., and G. Y. Ren (2011), Change in extreme temperature events frequency over mainland China during 1961–2008, *Clim. Res.*, *50*(1–2), doi:10.3354/cr01053.